

 Open access • Journal Article • DOI:10.1021/ACS.JPCC.6B09999

## 119Sn MAS NMR Study of the Interaction of Probe Molecules with Sn-BEA: The Origin of Penta- and Hexacoordinated Tin Formation — [Source link](#)

Alexander V. Yakimov, Yury G. Kolyagin, Søren Tolborg, Peter N. R. Vennestrøm ...+1 more authors

**Institutions:** Moscow State University, Technical University of Denmark

**Published on:** 06 Dec 2016 - Journal of Physical Chemistry C (American Chemical Society)

**Topics:** Tin, Adsorption and Isopropyl alcohol

Related papers:

- [Determination of the catalytically active oxidation Lewis acid sites in Sn-beta zeolites, and their optimisation by the combination of theoretical and experimental studies](#)
- [Tin-containing zeolites are highly active catalysts for the isomerization of glucose in water](#)
- [Active Sites in Sn-Beta for Glucose Isomerization to Fructose and Epimerization to Mannose](#)
- [Correlating Synthetic Methods, Morphology, Atomic-Level Structure, and Catalytic Activity of Sn-β Catalysts](#)
- [Sn-zeolite beta as a heterogeneous chemoselective catalyst for Baeyer – Villiger oxidations](#)

Share this paper:    

View more about this paper here: <https://typeset.io/papers/119sn-mas-nmr-study-of-the-interaction-of-probe-molecules-4rgzfk0w50>



## 119Sn MAS NMR Study of Probe Molecules Interaction with Sn-BEA: The Origin of Penta- and Hexacoordinated Tin Formation

Yakimov, Alexander V.; G. Kolyagin, Yury; Tolborg, Søren; Vennestrøm, Peter N. R.; Ivanova, Irina I.

*Published in:*

The Journal of Physical Chemistry Part C: Nanomaterials, Interfaces and Hard Matter

*Link to article, DOI:*

[10.1021/acs.jpcc.6b09999](https://doi.org/10.1021/acs.jpcc.6b09999)

*Publication date:*

2016

*Document Version*

Peer reviewed version

[Link back to DTU Orbit](#)

*Citation (APA):*

Yakimov, A. V., G. Kolyagin, Y., Tolborg, S., Vennestrøm, P. N. R., & Ivanova, I. I. (2016). 119Sn MAS NMR Study of Probe Molecules Interaction with Sn-BEA: The Origin of Penta- and Hexacoordinated Tin Formation. *The Journal of Physical Chemistry Part C: Nanomaterials, Interfaces and Hard Matter*, 120(49), 28083-28092. <https://doi.org/10.1021/acs.jpcc.6b09999>

---

### General rights

Copyright and moral rights for the publications made accessible in the public portal are retained by the authors and/or other copyright owners and it is a condition of accessing publications that users recognise and abide by the legal requirements associated with these rights.

- Users may download and print one copy of any publication from the public portal for the purpose of private study or research.
- You may not further distribute the material or use it for any profit-making activity or commercial gain
- You may freely distribute the URL identifying the publication in the public portal

If you believe that this document breaches copyright please contact us providing details, and we will remove access to the work immediately and investigate your claim.

## 119Sn MAS NMR Study of Probe Molecules Interaction with Sn-BEA: The Origin of Penta- and Hexacoordinated Tin Formation

Alexander Vyacheslavovich Yakimov, Yury G. Kolyagin, Søren Tolborg, Peter N. R. Vennestrøm, and Irina Igorevna Ivanova

*J. Phys. Chem. C*, **Just Accepted Manuscript** • DOI: 10.1021/acs.jpcc.6b09999 • Publication Date (Web): 21 Nov 2016

Downloaded from <http://pubs.acs.org> on December 1, 2016

### Just Accepted

“Just Accepted” manuscripts have been peer-reviewed and accepted for publication. They are posted online prior to technical editing, formatting for publication and author proofing. The American Chemical Society provides “Just Accepted” as a free service to the research community to expedite the dissemination of scientific material as soon as possible after acceptance. “Just Accepted” manuscripts appear in full in PDF format accompanied by an HTML abstract. “Just Accepted” manuscripts have been fully peer reviewed, but should not be considered the official version of record. They are accessible to all readers and citable by the Digital Object Identifier (DOI®). “Just Accepted” is an optional service offered to authors. Therefore, the “Just Accepted” Web site may not include all articles that will be published in the journal. After a manuscript is technically edited and formatted, it will be removed from the “Just Accepted” Web site and published as an ASAP article. Note that technical editing may introduce minor changes to the manuscript text and/or graphics which could affect content, and all legal disclaimers and ethical guidelines that apply to the journal pertain. ACS cannot be held responsible for errors or consequences arising from the use of information contained in these “Just Accepted” manuscripts.

1  
2  
3  
4  
5  
6  
7  
8  
9  
10  
11  
12  
13  
14  
15  
16  
17  
18  
19  
20  
21  
22  
23  
24  
25  
26  
27  
28  
29  
30  
31  
32  
33  
34  
35  
36  
37  
38  
39  
40  
41  
42  
43  
44  
45  
46  
47  
48  
49  
50  
51  
52  
53  
54  
55  
56  
57  
58  
59  
60

# $^{119}\text{Sn}$ MAS NMR Study of Probe Molecules Interaction with Sn-BEA: the Origin of Penta- and Hexacoordinated Tin Formation

*Alexander V. Yakimov<sup>a</sup>, Yury G. Kolyagin<sup>a,b</sup>, Søren Tolborg<sup>c,d</sup>, Peter N. R. Vennestrøm<sup>c</sup>, Irina I.*

*Ivanova\*<sup>a,b</sup>*

<sup>a</sup>Department of Chemistry, Lomonosov Moscow State University, Leninskie gory 1, Moscow,  
Russia.

<sup>b</sup>A.V. Topchiev Institute of Petrochemical Synthesis RAS, Moscow, Russia.

<sup>c</sup>Haldor Topsøe A/S, Haldor Topsøes Allé 1, DK-2800 Kgs. Lyngby.

<sup>d</sup>Technical University of Denmark, Department of Chemistry, Kemitorvet, DK-2800 Kgs.  
Lyngby.

## ABSTRACT

$^{119}\text{Sn}$  CPMG MAS NMR was applied to study the adsorption of acetonitrile, methanol, isopropanol, isobutanol and water over Sn-BEA enriched with  $^{119}\text{Sn}$  isotope. Two signals observed at ca. -422 and -443 ppm over dehydrated samples were attributed to tetraordinated framework tin sites with strong and weak Lewis acidity, respectively. The adsorption of

1  
2  
3 acetonitrile and methanol resulted in observation of pentacoordinated tin species, due to the  
4 formation of 1:1 adsorption complexes over both Sn-sites. Water adsorption led first to formation  
5 of pentacoordinated tin species, which were further converted into hexacoordinated species at  
6 longer reaction times. The latter transformation was found to be kinetically limited and was  
7 attributed to chemical interaction of tin sites with water, such as hydrolysis of Si-O-Sn bonds.  
8 The adsorption of isopropanol and isobutanol was accompanied by the formation of  
9 pentacoordinated Sn species in the case of weak sites and hexacoordinated Sn over sites with  
10 strong Lewis acidity, pointing to the possibility of dissociative adsorption of secondary alcohols  
11 over strong Sn-sites.  
12  
13  
14  
15  
16  
17  
18  
19  
20  
21  
22  
23  
24  
25

## 26 INTRODUCTION

27  
28 Sn-BEA zeotypes are promising heterogeneous catalysts for the conversion of sugars into  
29 methyl lactate<sup>1,2</sup>, the isomerization of glucose into fructose<sup>2-5</sup> and other important reactions such  
30 as Baeyer-Villiger oxidations<sup>6,7</sup>, Meerwein-Ponndorf-Verley-Oppenauer redox reactions<sup>8</sup>, ring-  
31 opening hydration of epoxides<sup>9</sup> etc. The exceptional catalytic properties of Sn-BEA are due to  
32 the combination of their Lewis acidity, the hydrophobic microenvironment around active sites  
33 and the ability to catalyze reactions in aqueous media. These properties make Sn-BEA especially  
34 relevant for biomass processing<sup>3,10,11</sup>.  
35  
36  
37  
38  
39  
40  
41  
42  
43  
44

45 It is generally accepted that tin atoms, which isomorphously substitute silicon in the zeolite  
46 framework, are the catalytically active sites in Sn-BEA<sup>10-12</sup>. However, the exact configuration of  
47 these sites has not yet been unambiguously determined although numerous techniques including  
48 quantum-chemical calculations<sup>13-16</sup>, DR-UV-Vis<sup>10</sup>, FTIR<sup>12,17-20</sup>, Mössbauer<sup>21</sup> and NMR  
49 spectroscopy<sup>21-24</sup> have been applied for this purpose.  
50  
51  
52  
53  
54  
55  
56  
57  
58  
59  
60

1  
2  
3 Among the different approaches, the application of probe molecules was shown to be the most  
4 fruitful for characterization of tin sites and their local environment<sup>8,11,12,14,17-20,23,25-30</sup>. Besides  
5 that, probe molecules were particularly useful in deducing the catalytic behavior by providing  
6 insights into the interaction of the active site with solvents, reactants, intermediates and products  
7 in reactions catalyzed by Sn-BEA. Different types of probe molecules including pyridine  
8 (Py)<sup>8,18,25</sup>, alkyl substituted pyridines<sup>8</sup>, ammonia<sup>14,18,26</sup>, deuterated acetonitrile (CD<sub>3</sub>CN)<sup>12,14,18-</sup>  
9 <sup>20,28</sup>, cyclohexanone<sup>8,30</sup>, alkyl substituted cyclohexanone<sup>8</sup>, dimethyl ether<sup>20</sup>, n-propylamine<sup>18</sup>,  
10 alcohols<sup>14,20,27</sup>, glucose<sup>23</sup> and water<sup>14,17,19,20,23,27</sup> were applied to characterize tin sites.  
11  
12

13  
14  
15 It should be noted that most studies involving probe molecules has been monitored by FTIR  
16 and TPD techniques<sup>8,12,17-20,26,28-30</sup>. Both these techniques provide comprehensive information on  
17 the state of the adsorbed probe molecule, indirectly providing information on the nature of the  
18 Sn-sites. The direct detection of Sn-sites interacting with probe molecules, however, is highly  
19 desirable to confirm the conclusions made from indirect methods as well as to get deeper insight  
20 into the structure and environment of Sn-sites interacting with different probe molecules.  
21  
22

23  
24  
25 This direct information can be best obtained by <sup>119</sup>Sn MAS NMR, a reliable method for  
26 probing <sup>119</sup>Sn nuclei and their environment<sup>5,21-24,31-33</sup>. In particular, <sup>119</sup>Sn MAS NMR allows for  
27 distinguishing between framework and extraframework tin nuclei formed during the synthesis,  
28 and provides information on tin coordination and T-site distribution in the material. Thus,  
29 extraframework SnO<sub>2</sub> species were shown to exhibit a signal at ca. -604 ppm, whereas  
30 tetrahedral Sn-sites were characterized by a number of signals in the range of -420 to -450 ppm  
31 when dehydrated and in the range of -650 to -730 ppm when hydrated<sup>24,26,31</sup>. However, recording  
32 of <sup>119</sup>Sn MAS NMR spectra of tin-containing zeolites with sufficient resolution is time-  
33 consuming, even in samples enriched with the <sup>119</sup>Sn isotope, due to low tin content in Sn-BEA  
34  
35  
36  
37  
38  
39  
40  
41  
42  
43  
44  
45  
46  
47  
48  
49  
50  
51  
52  
53  
54  
55  
56  
57  
58  
59  
60

1  
2  
3 (about 1-2 wt.%). Sophisticated NMR techniques help to overcome this problem. The use of  
4  
5 DNP-NMR is a good example<sup>21,22</sup>. In this case, the sensitivity is enhanced by 28 – 75 times by  
6  
7 exploiting the transfer of electron spin to the investigated nucleus. However, the specific  
8  
9 biradical molecules used as polarizing sources and solvents in combination with low-temperature  
10  
11 requirements (T = 100 K) do not allow the use of probe molecules for sample characterization.  
12  
13

14  
15 In the present work, we focus on applying a different strategy to optimize the use of <sup>119</sup>Sn  
16  
17 MAS NMR spectroscopy to study the interaction of Sn-sites with relevant probe molecules and  
18  
19 solvents. Specifically, the adaptation of the Carr-Purcell-Meiboom-Gill (CPMG) echo train  
20  
21 acquisition<sup>24</sup> used to enhance the signal-to-noise ratio combined with the application of <sup>119</sup>Sn  
22  
23 enrichment allows a detailed study of the interaction between Sn-sites and the probe molecules  
24  
25 within a reasonable timeframe. To assess the nature of different Sn sites and their reactivity,  
26  
27 acetonitrile, methanol, isopropanol, isobutanol and water are used as probe molecules.  
28  
29  
30  
31  
32  
33

## 34 EXPERIMENTAL METHODS

### 35 Synthesis of <sup>119</sup>Sn-BEA

36  
37 Labelled and unlabeled Sn-BEA materials were synthesized using non-seeding procedure  
38  
39 developed by Tolborg *et al.*<sup>34</sup>. In the case of unlabeled Sn-BEA, SnCl<sub>4</sub>·5H<sub>2</sub>O was used as a tin  
40  
41 source. For the preparation of the labeled tin source, metallic tin enriched with <sup>119</sup>Sn isotope was  
42  
43 dissolved in HCl as proposed by Renz *et al.*<sup>7</sup>. To avoid any undesirable oxidation states of tin, in  
44  
45 this work an excess of H<sub>2</sub>O<sub>2</sub> was added after dissolution of tin in HCl. The resulting tin source  
46  
47 thereby comprised an aqueous solution of H<sub>2</sub><sup>119</sup>SnCl<sub>6</sub>. The molar composition of the gel after the  
48  
49 addition of H<sub>2</sub><sup>119</sup>SnCl<sub>6</sub> was as described in 35. The details of preparation are given in Supporting  
50  
51  
52  
53  
54  
55  
56  
57  
58  
59  
60  
Information.

### Pretreatment conditions

As-synthesized samples were calcined under static conditions in air. A small amount of the sample powder was placed in a porcelain crucible in a muffle furnace. The calcination procedure involved: 1) heating to 550 °C, 4 °C/min; and 2) maintaining at 550 °C for 15 h.

The typical dehydration procedure before adsorption experiments involved treatment of the calcined sample at 250 °C under vacuum conditions for 3 h. In some experiments, the dehydration temperature was varied within 100 – 400 °C. To study the interaction of probe molecules with Sn-sites the molecules were adsorbed on the dehydrated sample at ambient temperature under vacuum conditions.

Acetonitrile, methanol, isopropanol, isobutanol and water were used as probe molecules. Acetonitrile and alcohols were dosed volumetrically in the range of 0.5 – 4 molecules per Sn atom. After the adsorption, the sample was transferred into the NMR rotor in a glovebox and sealed; then NMR spectrum was measured. The kinetics of the interaction of water with Sn-sites was studied directly in the NMR spectrometer after the adsorption of 4 molecules of water per Sn site at ambient temperature. The duration of the experiment was 67 hours. NMR spectra were acquired at 7 h intervals. After that, the sample was removed from the NMR spectrometer and kept in a closed rotor for 1 month whereafter a final NMR spectrum was measured.

### Characterization

X-ray diffraction analysis was performed on a D2 PHASER (Bruker) diffractometer, Tube power: 30 kV (10 mA). XRD patterns were measured in the range of  $2\theta = 5-50^\circ$  using filtered  $\text{CuK}\alpha$  ( $\lambda = 0.154060$  nm) radiation. SEM images were obtained with an electron microscope Hitachi TM-3030. The studies were carried out with an accelerating voltage of 15 kV; all samples were coated by Au before analysis.



<sup>119</sup>Sn MAS NMR spectra were recorded on AVANCE-II 400WB (Bruker) spectrometer (9.4 T). Triple-resonance 4 mm MAS DVT probe (BRUKER) was used for detection, MAS frequency being 12 kHz. Direct polarization combined with CPMG echo-train acquisition (DP-CPMG) was used as a main pulse sequence<sup>24</sup>. Spectra of dehydrated samples were measured applying 600 echoes without any proton decoupling. For the hydrated samples and samples with adsorbed probe molecules, high-power <sup>1</sup>H decoupling was used (SW-TPPM,  $\tau = 8 \mu\text{s}$ ,  $\phi = 15^\circ$ ,  $\omega(B_1) = 105 \text{ kHz}$ ) with only 25 echo in CPMG echo-train. For some samples, cross-polarization combined with CPMG echo-train acquisition (CP-CPMG) was applied. The <sup>119</sup>Sn NMR chemical shifts were calibrated by SnO<sub>2</sub> as secondary external reference (-604.3 ppm)<sup>36</sup>. For spectra processing, the TopSpin 2.1 (Bruker) program was used. Parameters of line shape were calculated using DMFIT software<sup>37</sup>. The main parameters of NMR experiments are given in Table S1 (Supporting Information).

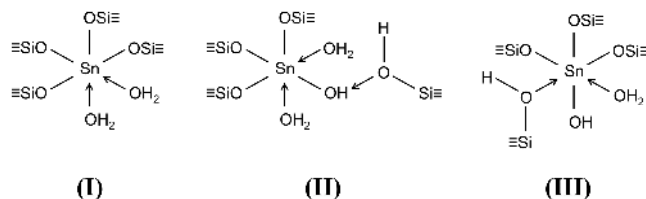
## RESULTS AND DISCUSSION

### Preparation and characterization of <sup>119</sup>Sn-BEA

Structural and morphological characteristics of Sn-BEA synthesized with labeled (<sup>119</sup>Sn-BEA) and unlabeled (Sn-BEA) tin sources are compared in Figs. S1 and S2 (Supporting Information). The results show that the different tin source did not affect the main characteristics of the samples. Overall, the labeled and unlabeled materials show the same structure, crystallinity, crystal size and morphology typical for Sn-BEA materials with Si/Sn = 200 ratio<sup>7,34</sup>.

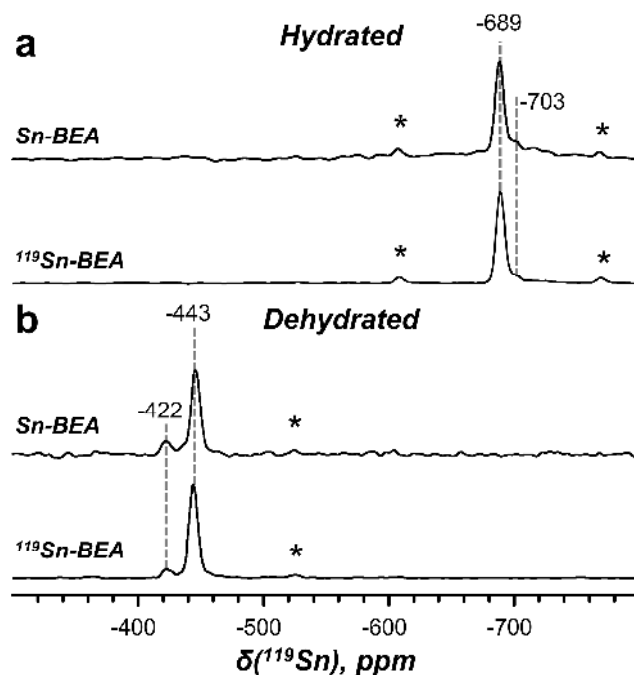
The <sup>119</sup>Sn MAS NMR spectra of calcined hydrated and dehydrated samples are illustrated in Fig. 1. Similar spectra are observed for <sup>119</sup>Sn-BEA and Sn-BEA samples, again pointing to an identical tin environment in labeled and unlabeled materials. In the spectra of the hydrated

samples two signals at ca. -689 and -703 ppm are observed. These signals were reported by other groups<sup>5,7,21,23,26,31</sup> and were attributed in the literature to hexacoordinated tin atoms, corresponding to “closed” Sn-sites with two water molecules in the first coordination sphere (I), “open” Sn-sites with two water molecules in the first coordination sphere (II) or “hydrolyzed-open” Sn-sites with one water molecule in the first coordination sphere (III)<sup>5,21,31</sup>:



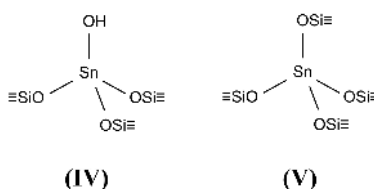
However, no unambiguous assignment of the resonances at ca. -689 and -703 ppm has been made so far.

It should be noted that no extra framework Sn or Sn connected with fluoride ions are present in the studied material as confirmed by the absence of a narrow peak at ca. -604 ppm<sup>7,26,38</sup> and -730 ppm<sup>23</sup> in the Sn-NMR spectrum, respectively.



1  
2  
3 **Figure 1.**  $^{119}\text{Sn}$  CP-CPMG MAS NMR spectra of hydrated (a) and  $^{119}\text{Sn}$  DP-CPMG MAS NMR  
4 spectra of dehydrated (b) Sn-BEA and  $^{119}\text{Sn}$ -BEA samples. Sidebands are marked with asterisks.  
5  
6  
7

8  
9 Upon dehydration of the samples, the signals corresponding to hexacoordinated tin disappear  
10 and two signals at -422 and -443 ppm appear in agreement with the literature data<sup>5,7,23,26</sup>.  
11 Bermejo-Deval *et al.*<sup>5</sup> have shown that the signal at ca. -420 ppm is amenable to cross-  
12 polarization. Based on the argumentation that this is the only site with a proton source in its  
13 proximity they assigned this signal to the so-called “open” site (IV); and as a consequence the  
14 signal at -443 ppm was assigned to “closed” sites (V):  
15  
16  
17  
18  
19  
20  
21  
22



30 In this work, we tried to confirm this assignment by applying cross-polarization conditions to  
31 our samples. However, we were not able to get any signal after sample dehydration at 250°C  
32 under vacuum (Fig. S3, Supporting Information). Comparing the pre-treatment conditions in our  
33 experiments with those applied in the work of Bermejo-Deval *et al.*<sup>5</sup>, it can be noticed that the  
34 authors used a dehydration pre-treatment at 120 °C, whereas 250 °C were used in our  
35 experiments. The decrease of the pre-treatment temperature of our sample to 150 °C revealed  
36 the appearance of signals at ca. -418 and -403 ppm (Fig. S3, Supporting Information). The  
37 intensity of these signals increased further when the temperature was decreased to 100 °C. This  
38 result confirms the presence of small amount of defect sites, however they are shown to  
39 condense and thereby disappear at higher dehydration temperatures. Since the signal at -422  
40 ppm was not amenable to cross-polarization in our experiments we cannot attribute it to “open”  
41 sites based on our data.  
42  
43  
44  
45  
46  
47  
48  
49  
50  
51  
52  
53  
54  
55  
56  
57  
58  
59  
60

1  
2  
3 At present, no direct correlation has been established between the different signals in the  
4 spectra of hydrated and dehydrated samples. The quantification of the NMR signals of hydrated  
5  $^{119}\text{Sn}$ -BEA sample obtained in this study points that the ratio between integral intensities of the  
6 signals at ca. -689 and -703 ppm corresponds to 87/13. For a dehydrated sample of  $^{119}\text{Sn}$ -BEA  
7 the ratio between the integrated signals at ca. -422 and -443 ppm is 15/85. This suggests that the  
8 signal obtained at ca. -703 ppm upon dehydration leads to the signal found at -422 ppm with a  
9 similar correlation existing for the signals at -689 and -443 ppm. Further studies are required,  
10 however, to confirm this hypothesis.  
11  
12  
13  
14  
15  
16  
17  
18  
19  
20  
21

### 22 Adsorption of acetonitrile

23  
24 The adsorption of acetonitrile is commonly used for the analysis of different Sn-sites and their  
25 Lewis acid strength<sup>12,17-20,33</sup>. In most cases, the adsorption of deuterated acetonitrile is monitored  
26 by FTIR spectroscopy. Additionally, some reports on the application of temperature programmed  
27 desorption (TPD) techniques are also available<sup>17,20</sup>. Application of this probe molecule allows for  
28 the differentiation between framework and extraframework tin sites<sup>12,20</sup>. Furthermore, based on  
29 the FTIR spectroscopy of deuterated acetonitrile displaying two bands at ca. 2316 and 2308  $\text{cm}^{-1}$ ,  
30 Boronat *et al.*<sup>12</sup> suggested the existence of two different framework sites in Sn-BEA, namely  
31 “open” and “closed” sites as mentioned earlier. The first band was assigned to the “open” Sn-site  
32 (IV) with three oxygen bonds connected to the zeolite framework and one to an -OH group. The  
33 second band was attributed to a closed site (V) with four oxygen bonds connected to the zeolite  
34 framework. In the same study it was shown that acetonitrile interacts more strongly with the site  
35 giving 2316  $\text{cm}^{-1}$  vibration and that there is a correlation between the acetonitrile adsorption band  
36 at 2316  $\text{cm}^{-1}$  and the catalytic activity in the Bayer-Villiger oxidation of adamantanone. The  
37 assignment of the two bands was however not supported by other (more recent) reports<sup>17,20</sup>. Roy  
38  
39  
40  
41  
42  
43  
44  
45  
46  
47  
48  
49  
50  
51  
52  
53  
54  
55  
56  
57  
58  
59  
60

1  
2  
3 *et al.* observed a single band at ca. 2310 cm<sup>-1</sup>, suggesting that the observation of the additional  
4  
5 line at 2316 cm<sup>-1</sup> was associated with solvent effects due to the presence or absence of additional  
6  
7 acetonitrile molecules in the vicinity<sup>20</sup>. Therefore, the information on the state of Sn atoms  
8  
9 during the adsorption of acetonitrile is highly desirable.  
10  
11

12  
13 In this study, we aimed to clarify the state of various Sn atoms during acetonitrile adsorption  
14  
15 by <sup>119</sup>Sn MAS NMR techniques. Different amounts of acetonitrile in the range of 0.5 – 4  
16  
17 molecules per tin atom were loaded onto the <sup>119</sup>Sn-BEA sample and the changes in the state of  
18  
19 tin were monitored by <sup>119</sup>Sn DP-CPMG/MAS NMR. The results are shown in Fig. 2.  
20  
21

22  
23 Upon adsorption of the first aliquot of acetonitrile (CH<sub>3</sub>CN/Sn = 0.5) both signals at -422 and -  
24  
25 443 ppm disappear. Instead, two new signals appear at -480 and -587 ppm with similar ratio of  
26  
27 integrated peak intensity as for the initial peaks at -422 and -443 ppm. This leads us to assume  
28  
29 that the weak signal at ca. -422 ppm shifts to -587 ppm, whereas the intensive resonance at -443  
30  
31 ppm yields a broad signal centered at -480 ppm. Upon further dosing of acetonitrile, the two sites  
32  
33 behave differently. The position of the weak signal at ca. -590 ppm practically does not change  
34  
35 with higher loadings (Fig. 2b). Conversely, the signal with the larger integral intensity continues  
36  
37 to move to higher field and reaches a chemical shift of -570 ppm at acetonitrile loadings of four  
38  
39 molecules per tin site. At the same time the line shape of the signal changes, becoming sharper  
40  
41 and well-defined. Further increase of loadings does not affect the peak position and shape.  
42  
43  
44  
45  
46  
47  
48  
49  
50  
51  
52  
53  
54  
55  
56  
57  
58  
59  
60

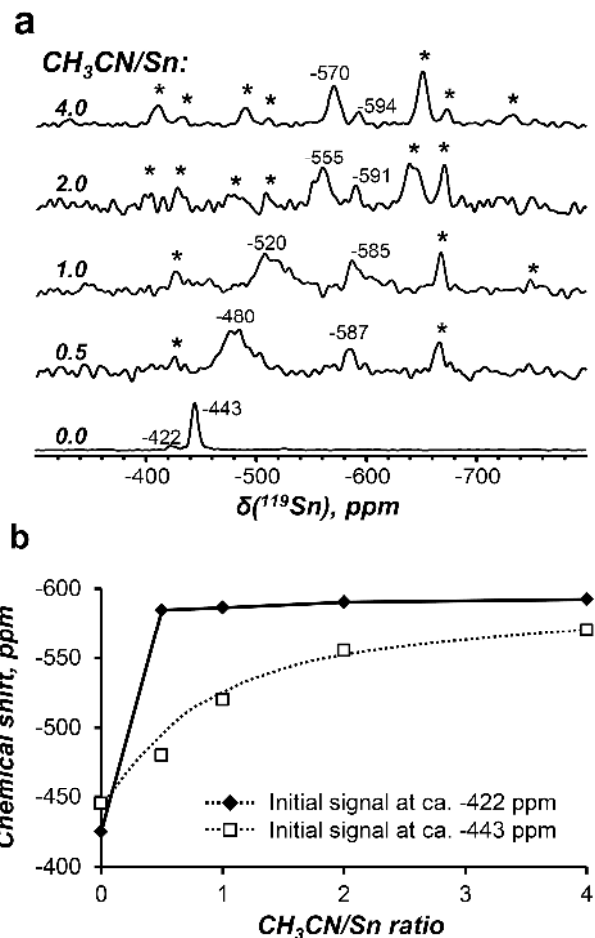


**Figure 2.**  $^{119}\text{Sn}$  DP-CPMG/MAS NMR spectra of dehydrated  $^{119}\text{Sn}$ -BEA zeolite before and after loading of acetonitrile in different amounts (a) and variation of chemical shift of signals at ca. -422 and -443 ppm with acetonitrile loading (b). Sidebands are marked with asterisks.

The variation of the chemical shift and the line shape with increased loadings could be due to fast exchange between different adsorption sites or between adsorbed and gaseous phases. This phenomenon has been described in detail by Bain<sup>39</sup>. At low loadings, the population of sites is rather low and only strong Sn-sites are permanently occupied. The rest of the adsorbate can exchange between the adsorbed and gaseous phases or between the different weak sites related to and not related to tin (for instance, weak Sn Lewis sites and silanol groups). As a result, of this exchange a weighted average of the chemical shift between occupied and pristine Sn-sites is

1  
2  
3 observed. At high loadings, all sites become occupied and the chemical shift observed after  
4  
5 saturation corresponds to Sn-sites with adsorbed acetonitrile (Fig. 2b).  
6  
7

8 The position and parameters of the shape of NMR signals at ca. -570 and -594 ppm are similar  
9  
10 to those calculated for pentacoordinated closed Sn-sites by Wolf *et al.*<sup>21,31</sup>. Although their  
11  
12 calculations were performed for the adsorption of water molecules, the chemical shift should not  
13  
14 change drastically in the case of acetonitrile adsorption. No lines around ca. -703 ppm are  
15  
16 observed in the NMR spectra even at high loadings, suggesting that no hexacoordinated Sn is  
17  
18 formed upon the adsorption of acetonitrile. Thus, only one molecule of acetonitrile binds to the  
19  
20 Sn-sites despite the high dosage of up to 4 molecules of acetonitrile per Sn site. These findings  
21  
22 confirm the conclusion on equimolar stoichiometry of acetonitrile adsorption made by Harris *et*  
23  
24 *al.*<sup>18</sup> using FTIR spectroscopy of adsorbed deuterated acetonitrile. Furthermore, our results  
25  
26 suggest that the Sn-site that gives a signal at -422 ppm binds acetonitrile stronger than the site at  
27  
28 -443 ppm, which is in excellent agreement with previous observations made by the groups of  
29  
30 Corma<sup>12</sup> and Davis<sup>5</sup>. In this contribution, we, however, cannot comment on the assignment of  
31  
32 these signals to “open” and “closed” sites, respectively.  
33  
34  
35  
36  
37

### 38 Adsorption of alcohols

39  
40 Alcohols, especially methanol, are used as solvents and often substrates in reactions catalyzed  
41  
42 by Sn-BEA<sup>1,30,40</sup>, making it essential to study adsorption of alcohols over Sn-BEA in order to  
43  
44 understand the state of tin directly during the catalytic reaction mixture. Roy *et al.*<sup>20</sup> studied the  
45  
46 adsorption of 2-methyl-2-propanol and diethyl ether with Sn-BEA using TPD-TGA techniques.  
47  
48 It was shown that 2-methyl-2-propanol and diethyl ether interact differently with Sn-BEA.  
49  
50 Diethyl ether yields a 1:1 adsorption complex with tin and desorbs intact. On the contrary, 2-  
51  
52 methyl-2-propanol gives coverages of more than twice the tin content in the analyzed sample.  
53  
54  
55  
56  
57  
58  
59  
60

1  
2  
3 Besides that, part of 2-methyl-2-propanol molecules desorbs as butene and water. This work  
4 impelled us to monitor the adsorption of alcohol molecules with smaller (methanol) and larger  
5 sizes (isopropanol, isobutanol).  
6  
7  
8  
9

10 Fig. 3a shows the comparison of  $^{119}\text{Sn}$  DP-CPMG/MAS NMR spectra recorded after  
11 adsorption of alcohol molecules over dehydrated  $^{119}\text{Sn}$ -BEA together with the spectrum obtained  
12 for acetonitrile. In all the experiments, the adsorbate loadings were close to 4 molecules per Sn  
13 atom. The results show that the adsorption of methanol gives a spectrum very similar to that of  
14 acetonitrile: two lines corresponding to pentacoordinated Sn-sites are observed at -576 and -588  
15 ppm.  
16  
17  
18  
19  
20  
21  
22  
23

24 In the case of isopropanol and isobutanol, a slightly different picture is observed (Fig. 3a). In  
25 particular, only intensive NMR line is detected in the range of -582 to -586 ppm, while the weak  
26 resonance at ca. -590 ppm corresponding to the adsorption on sites with strong acidity is not  
27 seen. To further assess this behavior, the adsorption of small aliquots of isobutanol was  
28 monitored. The adsorption of small amounts of isobutanol reveals the presence of this signal  
29 (Fig. 3b) at ca. -589 ppm, however the increase of isobutanol loadings leads to its vanishing. The  
30 decrease of the signal at ca. -589 ppm is accompanied by the appearance of a small resonance at  
31 ca. -703 ppm, which is more pronounced with cross-polarization. The latter signal can be  
32 attributed to hexacoordinated tin atoms. The reasons for the observation of hexacoordinated tin  
33 as a result of interaction of secondary alcohols with strong tin sites will be discussed later.  
34  
35  
36  
37  
38  
39  
40  
41  
42  
43  
44  
45  
46  
47  
48  
49  
50  
51  
52  
53  
54  
55  
56  
57  
58  
59  
60



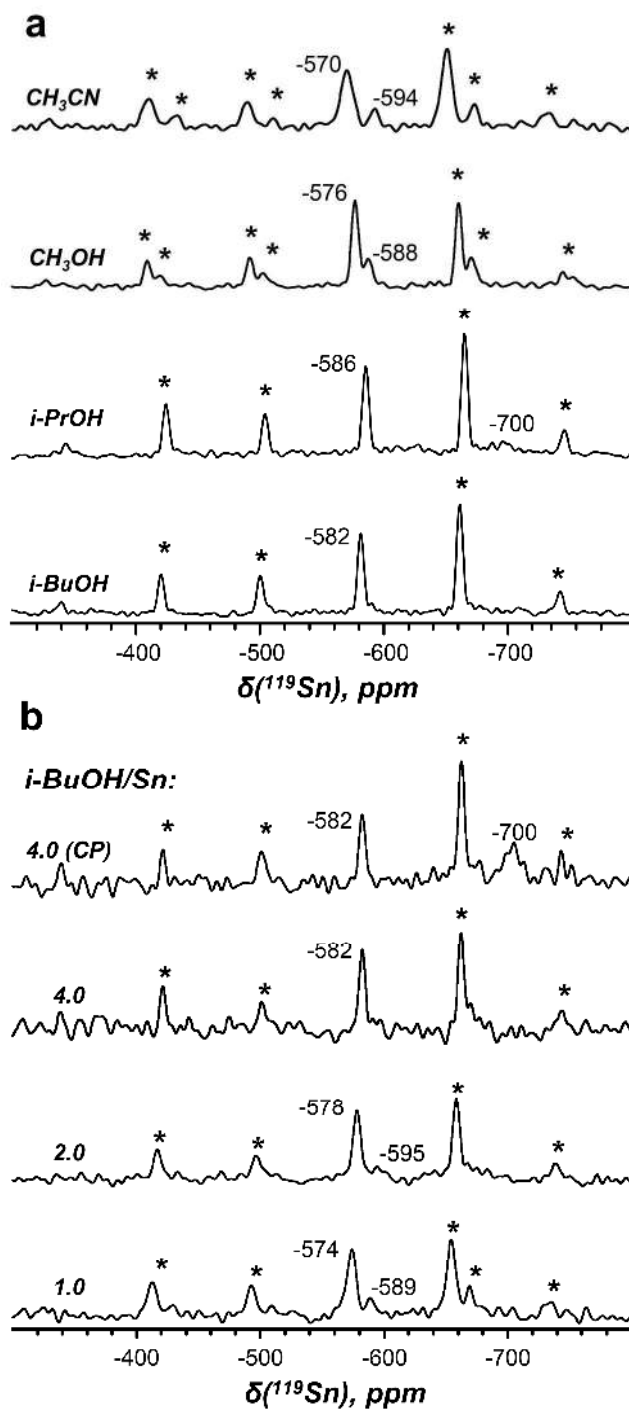


**Figure 3.**  $^{119}\text{Sn}$  DP-CPMG MAS NMR spectra of acetonitrile, methanol, isopropanol and isobutanol adsorbed over  $^{119}\text{Sn}$ -BEA in the ratio of adsorbate/Sn = 4(a); variation of  $^{119}\text{Sn}$  DP-CPMG MAS NMR spectra with isobutanol loadings (b). Spectrum 4.0 (CP) is recorded using  $^{119}\text{Sn}$  CP-CPMG MAS NMR. Sidebands are marked by asterisks.

### Adsorption of water

The interaction with water is of special interest, since aqueous phase reactions are an integral part of biomass processing. Furthermore, even when alcohol is used as solvent, water is often present in the reaction mixture either as an impurity or as a by-product<sup>30,40</sup>. Finally, tin sites in the catalyst are usually in a hydrated state as the catalyst is seldom dried prior to use. Changes in catalysts structure as a result of hydration could be responsible for a number of observations responsible for catalytic activity. Therefore, one cannot consider tin sites in Sn-BEA catalysts inseparably from water in most reactions.

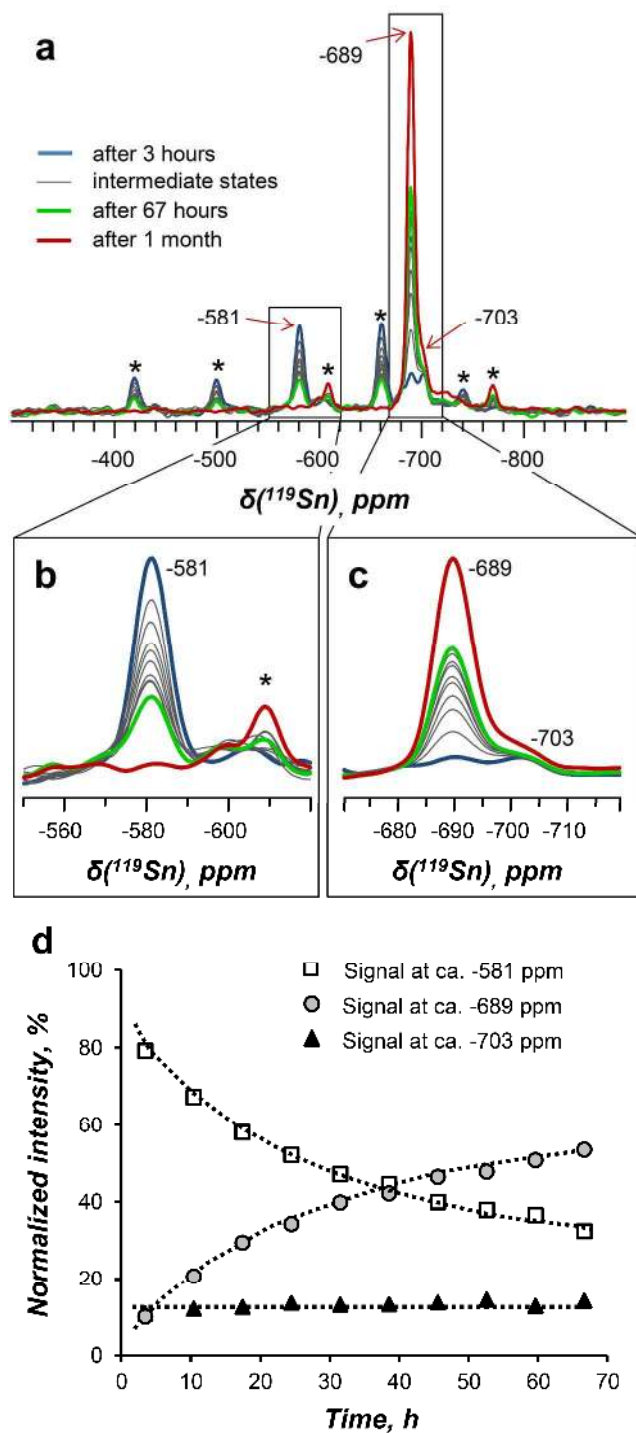
The adsorption of water on Sn-BEA has been studied in several reports<sup>17,19,20,23,27,31</sup>. The comparison of the isotherms of water adsorption over various hydrophobic zeolites obtained in fluoride media showed that the amount of water adsorbed over Sn-BEA was higher than on Ti-BEA and Si-BEA by a factor of 2<sup>27</sup>. Theoretic calculations suggested stronger adsorption of water on Sn-BEA as compared to other substrates, such as NH<sub>3</sub>, alcohols and acetonitrile<sup>13-16</sup>. This was also confirmed experimentally<sup>17,19,20,23</sup>. Furthermore, Courtney *et al.*<sup>17</sup> revealed that the adsorption of water is accompanied by the formation of SiOH groups. The process was found to be very slow (requiring several days), nevertheless shown to occur even at mild relative humidity and ambient temperature. At 98 °C in liquid water SiOH formation was found to happen in less than 1 h. These silanol groups were stable at temperatures as high as 400 °C and found to condense in the range of 400 – 700 °C. Based on these results the authors concluded that dissociative adsorption of water occurs over Sn-BEA. Additionally, it was found out that the extent of hydroxylation is proportional to the Sn content. This conclusion was further supported by the results of Otomo *et al.*<sup>19</sup> by studying the ion exchange of Sn-BEA with different alkali

1  
2  
3 cations. They found out that not only “open” but also “closed” sites without adjacent silanol  
4 groups could be ion-exchanged through the hydrolysis of Si-O-Sn bonds. In the case of Cs<sup>+</sup>, K<sup>+</sup>  
5 and NH<sub>4</sub><sup>+</sup> cations, the ratio of cation/Sn reached 1, indicating that all Sn-sites were fully  
6 converted into “open” sites and exchanged. This is a relevant finding, as the exchange with alkali  
7 metal salts has been shown to affect the catalytic activity and selectivity in several reactions;  
8 either facilitating epimerization (instead of isomerization) of sugars or changing the reaction  
9 pathway from a retro-aldol mechanism (yielding methyl lactate and similar products) to a β-  
10 dehydration mechanism facilitating the formation of newly discovered bio-monomers<sup>33,41,42</sup>.

11  
12  
13 The state of Sn during hydration was studied by <sup>119</sup>Sn MAS NMR by Hwang *et al.*<sup>23</sup>. The  
14 authors observed mainly hexacoordinated tin after adsorption of two molecules of water per tin  
15 atom. Very small signals attributed to pentacoordinated tin were also detected.

16  
17  
18 To get deeper insight into the interaction of water molecules with the Sn-sites present in Sn-  
19 BEA, we studied the kinetics of water adsorption. The dehydrated sample was exposed to a H<sub>2</sub>O  
20 aliquot corresponding to H<sub>2</sub>O/Sn = 4.0 and the development in NMR signals was monitored with  
21 time. Fig. 4 shows the NMR spectra obtained before and after the exposure to water. After three  
22 hours of exposure three signals have appeared: an intensive signal at ca. -581 ppm  
23 (pentacoordinated Sn-sites) and two weak signals at ca. -689 and -703 ppm (hexacoordinated Sn-  
24 sites). In agreement with earlier observations, the small signal at ca. -703 ppm arises from the  
25 signal at ca. -422 ppm in the dehydrated sample, whereas the signals at -580 and -689 ppm  
26 originate from the signal at ca. -443 ppm. The analysis of the intensities of the lines suggests that  
27 the Sn sites with strong acidic character observed at -422 ppm in the dehydrated sample give  
28 predominantly hexacoordinated sites already at the initial steps of the hydration. The small signal  
29 observed in the range of -590 to -600 ppm, could be attributed to pentacoordinated tin, but it is  
30  
31  
32  
33  
34  
35  
36  
37  
38  
39  
40  
41  
42  
43  
44  
45  
46  
47  
48  
49  
50  
51  
52  
53  
54  
55  
56  
57  
58  
59  
60

on the level of the noise. On the contrary, Sn-sites associated with weak acidity (signal at ca. -443 ppm in the dehydrated sample) are converted mostly to pentacoordinated tin, giving the signal at ca. -581 ppm.



1  
2  
3 **Figure 4.** Variation of  $^{119}\text{Sn}$  DP-CPMG MAS NMR spectra of  $^{119}\text{Sn}$ -BEA with time (a) after  
4 exposure to water ( $\text{H}_2\text{O}/\text{Sn} = 4$ ). The regions from -550 to -625 ppm (b) and -675 – -710 ppm (c)  
5 are highlighted. Variation of normalized integrated intensity of  $^{119}\text{Sn}$  MAS NMR signals at ca. -  
6 581, -689 and -703 ppm with time of exposure to water (d). Sidebands are marked as asterisks.  
7  
8  
9

10  
11  
12  
13  
14 The changes in signals intensities during 67 h of experiment are shown in Fig. 4d. The results  
15 show that the intensity of the signal at ca. -581 ppm decreases down to 32 %, whereas the  
16 intensity of the signal at ca. -690 ppm increases up to 54 %. The signal at ca. -703 ppm remains  
17 at the level of 11-14% during the whole duration of experiment (Fig. 4d).  
18  
19  
20  
21

22  
23 After 1 month, the signal at ca. -581 ppm disappears completely, whereas the two signals at ca.  
24 -689 and -703 ppm remain (Fig. 4) and the spectrum becomes very similar to those of fully  
25 hydrated samples (for comparison see Figs. 1 and 4, red spectrum). The ratio between the  
26 intensities of signals at ca. -689 and -703 ppm is 86/14, which is very close to hydrated sample  
27 (87/13).  
28  
29  
30  
31  
32  
33

34  
35 The analysis of CP-CPMG MAS NMR spectra obtained over  $^{119}\text{Sn}$ -BEA sample after  
36 adsorption of water (Fig. S4) points that pentacoordinated Sn sites (-581 ppm) does not show  
37 any signal when cross-polarization is applied. On the contrary, the signals at ca. -689 and -703  
38 ppm attributed to hexacoordinated tin are amenable to cross-polarization. The latter observation  
39 can be accounted for by the formation of hydrolyzed open Sn sites (III).  
40  
41  
42  
43  
44  
45

46  
47 It is important to note that dehydration of the sample after adsorption of water results in  
48 complete restoration of the spectrum of dehydrated sample (Fig. S5). These observations suggest  
49 that the changes observed during hydration/dehydration are fully reversible.  
50  
51  
52

53  
54 To summarize, Sn-sites with strong Lewis acidic character (-422 ppm) and weak Lewis acidic  
55 character (-443 ppm) show different behavior upon interaction with water. The strong sites react  
56  
57  
58  
59  
60

1  
2  
3 faster than the time-scale of our experiment, resulting in the immediate transformation of  
4  
5 tetracoordinated tin into the hexacoordinated state. On the contrary, weak sites are first  
6  
7 transformed into the pentacoordinated state followed by very slow (up to one month at ambient  
8  
9 temperature) rearrangement into hexacoordinated state. These observations are in line with  
10  
11 previous findings<sup>17,19</sup> and point to dissociative adsorption of water leading to hydrolysis of Si-O-  
12  
13 Sn bounds. Furthermore, our results suggest that in fully hydrated samples all Sn-sites are  
14  
15 hydrolyzed.  
16  
17  
18

## 19 IMPLICATIONS

20  
21  
22 <sup>119</sup>Sn CPMG MAS NMR of adsorbed probe molecules revealed the existence of two different  
23  
24 framework Sn-sites with different adsorption properties:  
25

- 26 - Sn-sites associated with strong Lewis acidity and characterized by an NMR signal at ca. -  
27  
28 422 ppm;  
29
- 30 - Sn-sites with lower acidity and an NMR signal located at -443 ppm.  
31  
32

33  
34 Our data do not allow for these sites to be attributed as “open” or “closed” as it was proposed in  
35  
36 other reports<sup>5,12</sup>, since none of the signals observed is amenable to cross-polarization. We  
37  
38 suppose that the origin of different signals is more likely due to the different locations in the  
39  
40 framework of Sn-BEA, as it has also been suggested by theoretical calculations<sup>31</sup>. According to  
41  
42 our data, the ratio between these sites can be changed by adjusting of synthesis conditions,  
43  
44 variation of tin content<sup>35</sup> and pretreatment conditions<sup>24</sup>.  
45  
46  
47  
48

49 **Table 1.** Parameters of NMR line shape ( $\delta_{\text{iso}}$ ,  $\Omega$  and  $\kappa$ ) of signals corresponding to  
50  
51 pentacoordinated tin sites in Sn-BEA bonded to different probe molecules.  
52

Expected structure of adsorption	Type of	NMR parameter	Reference
----------------------------------	---------	---------------	-----------

complex	Sn-site	$\delta_{\text{iso}}^{\text{a}}$ , ppm	$\Omega$ (span), ppm	$\kappa$ (skew)	
	-	-575	393	-0.47	21 <sup>b</sup>
(H <sub>2</sub> O)Sn <sup>V</sup> (OSi≡) <sub>4</sub>	-	-560...-585 <sup>c</sup>	360...420 <sup>c</sup>	n.d.	31 <sup>b</sup>
	Weak	-581	360 ± 20	-0.8 ± 0.2	
(CH <sub>3</sub> CN)Sn <sup>V</sup> (OSi≡) <sub>4</sub>	Strong	-594	415 ± 30	-0.8 ± 0.2	
	Weak	-570	390 ± 20	-0.7 ± 0.2	
(CH <sub>3</sub> OH)Sn <sup>V</sup> (OSi≡) <sub>4</sub>	Strong	-588	375 ± 35	-0.8 ± 0.2	this work <sup>d</sup>
	Weak	-576	390 ± 20	-0.7 ± 0.3	
( <i>i</i> -PrOH)Sn <sup>V</sup> (OSi≡) <sub>4</sub>	Weak	-586	400 ± 25	-0.8 ± 0.2	
( <i>i</i> -BuOH)Sn <sup>V</sup> (OSi≡) <sub>4</sub>	Weak	-582	415 ± 25	-0.7 ± 0.3	

<sup>a</sup> Isotropic chemical shift.

<sup>b</sup> Theoretical data.

<sup>c</sup> Approximate values from Fig. S29 in 31.

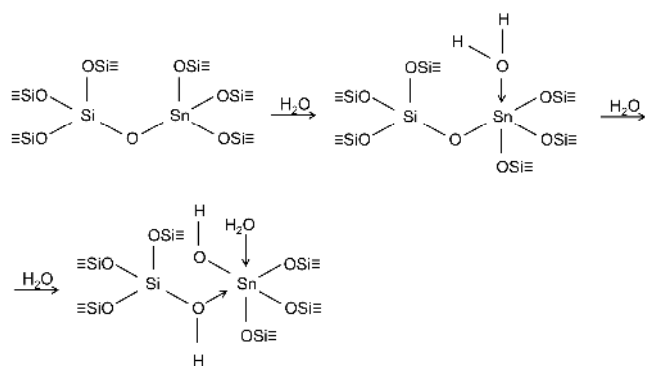
<sup>d</sup> Experimental data, 4 probe molecules per one Sn atom.

### Sn-sites with weak Lewis acidity (-443 ppm)

The major fraction of sites, corresponding to approximately ~85% of the Sn sites in the samples studied (Fig. 1), is characterized by relatively weak Lewis acidity. The adsorption of acetonitrile and alcohols over these sites reveals that Sn atoms change their coordination and become pentacoordinated (Fig. 3), which accounts for the adsorption of one probe molecule per tin site in accordance with other reports<sup>18,20</sup>. Acetonitrile show very weak adsorption over these Sn-sites. The position of Sn signal is changing from -480 to -570 ppm upon variation of CH<sub>3</sub>CN loadings from 0.5 to 4 molecules per Sn site (Fig. 2), which points to fast exchange between different adsorption sites, related and not related to tin. The alcohol molecules show stronger interaction with Sn sites, the exchange process is not detected and the signal at ca. -570 ppm appears already at low loadings (Fig. 3b). The analysis of the chemical shifts and parameters of NMR line shape of the signal at ca. -580 ppm, observed for all adsorbates (Table 1) point to

similar features for acetonitrile and alcohols at higher loadings. We therefore conclude that the structure of adsorption complexes is similar in all the cases.

A different situation is observed in the case of water adsorption. At the early steps of the interaction with water, the Sn-sites responsible for the NMR signal at -443 ppm adsorb one molecule of water leading to the formation of pentacoordinated Sn as confirmed by the appearance of the line at ca. -581 ppm. However, after several hours pentacoordinated Sn-sites start to convert into hexacoordinated sites. This transformation is slow and kinetically limited. The complete transformation requires more than 3 weeks, which is in line with the results obtained by Courtney *et al.*<sup>17</sup>, who showed that adsorption of water is accompanied by the rupture of Si-O-Sn bond and formation of SiOH groups. These SiOH groups were shown to be slightly acidic and exchangeable with alkali cations<sup>19</sup>. Furthermore, this work points to the formation of SnOH as confirmed by CP-CPMG MAS NMR spectra showing the intensive signal for hexacoordinated Sn at ca. -689 ppm (Fig. S4). Putting together our results with the literature data<sup>17,19</sup> one can conclude that the observation of hexacoordinated Sn-sites is due to dissociative adsorption of water over these sites:



**Scheme 1.** Dissociative adsorption of water over tin sites in Sn-BEA.



1  
2  
3 During this process the rupture of Si-O-Sn bonds occurs and the Sn-site becomes more flexible  
4 and able to accommodate additional water molecule leading to the observation of  
5 hexacoordinated tin.  
6  
7  
8

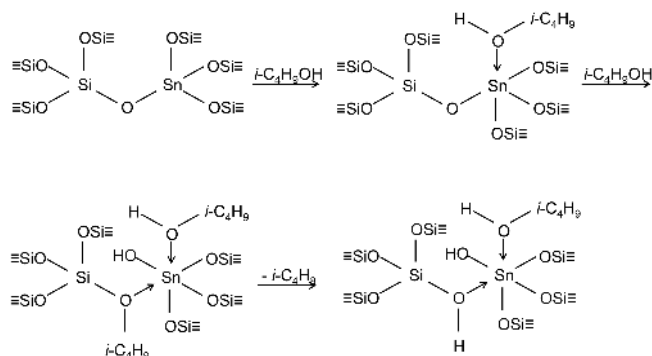
9  
10 The hydrolysis of Si-O-Sn bonds explains why the formation of 6-coordinated tin is observed  
11 only in the case of adsorption of water and not in the case of acetonitrile and alcohols. One can  
12 suppose that tin is not stable in the octahedral surrounding in the zeolite framework due to steric  
13 hindrance. Consequently, high energy is required to transform rather stable distorted  
14 pentacoordinated tin into hexacoordinated tin. The dissociative adsorption of water is slow over  
15 weak Sn-sites at ambient temperature and mild relative humidity, but it can be accelerated when  
16 the temperature is raised and the humidity increased<sup>17</sup>.  
17  
18  
19  
20  
21  
22  
23  
24  
25

#### 26 27 Sn-sites with strong Lewis acidity (-422 ppm)

28  
29 Monitoring the fate of the signal at ca. -422 ppm during the adsorption of different probe  
30 molecules points to a stronger interaction with these sites compared to those observed at ca. -443  
31 ppm. In the case of acetonitrile, even very small loadings give the line at ca. -580 ppm,  
32 corresponding to pentacoordinated Sn (Fig. 2). No exchange process with other sites is observed,  
33 pointing to strong adsorption over the. -422 ppm sites. Furthermore, the dissociative adsorption  
34 of water occurs in a few hours over -422 ppm Sn-sites at ambient temperature (Fig. 4), whereas it  
35 requires several weeks in the case of -443 ppm sites. Finally, secondary alcohols (isopropanol  
36 and isobutanol) reveal the formation of hexacoordinated tin upon the adsorption over -422 ppm  
37 Sn-sites at high loadings (Fig. 3), whereas only pentacoordinated tin was observed in the case of  
38 -443 ppm Sn-sites.  
39  
40  
41  
42  
43  
44  
45  
46  
47  
48  
49  
50  
51  
52

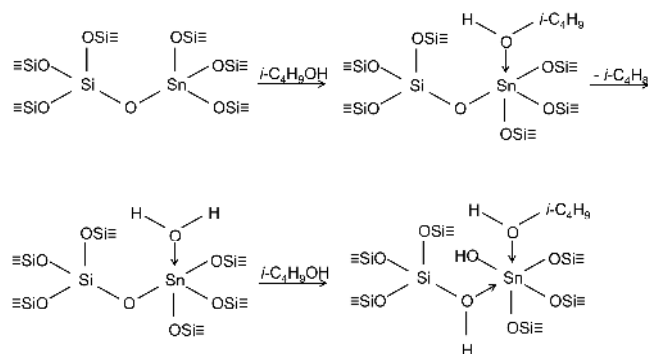
53 The latter observation requires additional discussion. As it has been shown above, the  
54 formation of hexacoordinated Sn-sites is an activated process and requires the rupture of Si-O-Sn  
55  
56  
57  
58  
59  
60

bonds. In the case of interaction with secondary alcohols, this rupture can take place via dissociative adsorption and formation of alkoxy groups attached to silicon atoms and Sn-OH groups:



**Scheme 2.** Dissociative adsorption of isobutanol over tin sites in Sn-BEA.

The alkoxy groups can further decompose into corresponding olefin and Si-OH group. Another possibility involves dehydration of secondary alcohols over Sn-sites yielding an olefin and water and dissociative adsorption of water over Sn-site:



**Scheme 3.** Dehydration of isobutanol over tin site in Sn-BEA followed by dissociative adsorption of water formed.

The decomposition of alcohols into olefins and water over Sn-sites has been observed previously<sup>20</sup>. Roy *et al.* observed dissociative adsorption of 2-methyl-2-propanol over Sn-BEA leading to evolution of butene and water during TPD-TGA experiments. The amount of butene and water desorbed was close to Sn content in the sample. Our results confirm this findings but

1  
2  
3 suggest that only Sn sites with strong Lewis acid strength (-422 ppm) are involved in this type of  
4  
5 interaction at ambient temperature. One can speculate that at higher temperature, weaker tin sites  
6  
7 can also be involved in this interaction.  
8  
9

10 It should be noted that the present data as well as the literature data<sup>17</sup> do not allow to  
11  
12 distinguish between two possible pathways: 1) dissociative adsorption of alcohols (Scheme 2) or  
13  
14 2) dehydration of alcohols / dissociative adsorption of water (Scheme 3). Further experiments are  
15  
16 needed to verify this.  
17  
18

19 The results obtained are useful for understanding the effect of solvents on the catalytic  
20  
21 properties, since they clearly demonstrate that the chosen solvent can modify the active Sn-site  
22  
23 even at moderate temperatures. As most reactions involving Sn-BEA and the conversion of sugar  
24  
25 substrates are currently being performed in either water or using smaller alcohol solvents  
26  
27 (methanol, ethanol), the current study shows that it is difficult to investigate the system without  
28  
29 taking into account interaction with the solvent. Additionally, as it is shown here that water even  
30  
31 at ambient temperature will modify the catalyst, this naturally has relevance for the catalytic  
32  
33 system, as also pointed out by Corma *et al.*<sup>43</sup>, since age and general history of the tested Sn-BEA  
34  
35 are often not reported.  
36  
37  
38  
39  
40  
41  
42

## 43 CONCLUSIONS

44 Probing of Sn-sites in Sn-BEA by <sup>119</sup>Sn CPMG MAS NMR of adsorbed acetonitrile, methanol,  
45  
46 isopropanol, isobutanol and water reveals two sites with different adsorption properties: 1) Sn-  
47  
48 sites with strong Lewis acidity, characterized by the NMR line at ca. -422 ppm in dehydrated  
49  
50 state; and 2) Sn-sites with lower Lewis acidity at -443 ppm. In the samples studied, the major  
51  
52 fraction of Sn-sites (~85%) could be attributed to the latter.  
53  
54  
55  
56  
57  
58  
59  
60

1  
2  
3 Interaction of both tin sites with acetonitrile and methanol leads to formation of only  
4  
5 pentacoordinated tin species, which is confirmed by the appearance of two well-defined NMR  
6  
7 signals at ca. -570 and -594 ppm corresponding to the sites responsible for the -443 and -422  
8  
9 ppm signals, respectively. Observation of pentacoordinated species accounts for the formation of  
10  
11 1:1 adsorption complexes. Acetonitrile shows weak adsorption especially over Sn-sites,  
12  
13 characterized by NMR signal at ca. -443 ppm. The position of the NMR signal is found to vary  
14  
15 from -480 to -570 ppm upon changing of CH<sub>3</sub>CN loadings from 0.5 to 4 molecules per Sn site,  
16  
17 which points to fast exchange between different adsorption sites, related and not related to tin.  
18  
19 This exchange process is not observed for the signal at -422 ppm, pointing to stronger adsorption  
20  
21 over this site. Analysis of chemical shifts and the NMR line shape shows similar local  
22  
23 surroundings of the adsorbed pentacoordinated tin complexes for the different probe molecules.  
24  
25  
26  
27

28  
29 Interaction of tin sites with water initially leads to the formation of pentacoordinated tin. But  
30  
31 unlike for acetonitrile and methanol, water enables the transformation of tin sites into  
32  
33 hexacoordinated state, evidenced by the observation of the NMR lines at ca. -689 and -703 ppm.  
34  
35 This transformation occurs at ambient temperatures in several hours in the case of the strong  
36  
37 sites (-422 ppm), but requires several weeks for weak sites (-443 ppm), indicating that the  
38  
39 process is kinetically limited by the chemical interaction. We suggest that the formation of  
40  
41 hexacoordinated tin is a result of the hydrolysis of Si-O-Sn bonds, occurring already at ambient  
42  
43 temperatures.  
44  
45  
46  
47

48 Interaction with isopropanol and isobutanol shows the formation of pentacoordinated Sn  
49  
50 species over weak sites and hexacoordinated Sn over strong sites, pointing to the possibility of  
51  
52 dissociative adsorption of secondary alcohols over the Sn-sites with strong Lewis acidity.  
53  
54  
55  
56  
57  
58  
59  
60

1  
2  
3 The results obtained could have practical implications in understanding the effect of solvents  
4 on the catalytic properties, since they clearly demonstrate that solvents can modify the active Sn-  
5  
6  
7  
8 site.  
9  
10  
11  
12  
13  
14  
15  
16  
17  
18  
19  
20  
21  
22  
23  
24  
25  
26  
27  
28  
29  
30  
31  
32  
33  
34  
35  
36  
37  
38  
39  
40  
41  
42  
43  
44  
45  
46  
47  
48  
49  
50  
51  
52  
53  
54  
55  
56  
57  
58  
59  
60

1  
2  
3 ASSOCIATED CONTENT  
4  
5

6 **Supporting Information.** Details of preparation and characterization of Sn-BEA, main  
7 acquisition parameters in NMR spectra, XRD and SEM images of the product obtained,  $^{119}\text{Sn}$   
8 DP- and CP-CPMG/MAS NMR spectra of hydrated and dehydrated samples. This material is  
9 available free of charge via the Internet at <http://pubs.acs.org>.  
10  
11  
12  
13  
14  
15

16  
17 AUTHOR INFORMATION  
1819  
20 **Corresponding Author**  
2122  
23 \*Irina I. Ivanova  
2425  
26 Laboratory of kinetics and catalysis, Department of Chemistry, Lomonosov MSU  
2728  
29 119991, Moscow, Leninskie gory, 1 bld. 3.  
3031  
32  
33 Tel.: +7(495)939-35-70  
3435  
36 e-mail: [IIvanova@phys.chem.msu.ru](mailto:IIvanova@phys.chem.msu.ru)  
37  
3839 **Author Contributions**  
4041  
42 The manuscript was written through contributions of all authors. All authors contributed equally.  
43  
4445  
46 ACKNOWLEDGMENT  
4748  
49 The authors thank the Russian Science Foundation for the financial support (grant 14-23-  
50 00094). Alexander V. Yakimov gratefully acknowledges Haldor Topsøe A/S for a PhD  
51 fellowship. Søren Tolborg is funded by the Bio-Value platform under the Danish Council for  
52  
53  
54  
55  
56  
57  
58  
59  
60

1  
2  
3 Strategic Research and The Danish Council for Technology and Innovation (Case no. 0603-  
4  
5 00522B).  
6  
7

#### 8 9 ABBREVIATIONS 10

11 DNP, dynamic nuclear polarization; CPMG, sequence containing a number of refocusing  
12 pulses developed by Carr-Purcell-Meiboom-Gill; CP-CPMG, cross-polarization sequence  
13 combined with CPMG echo train acquisition; DP-CPMG, direct polarization (90°-pulse)  
14 combined with CPMG echo train acquisition.  
15  
16  
17  
18  
19  
20  
21  
22  
23  
24  
25  
26  
27  
28  
29  
30  
31  
32  
33  
34  
35  
36  
37  
38  
39  
40  
41  
42  
43  
44  
45  
46  
47  
48  
49  
50  
51  
52  
53  
54  
55  
56  
57  
58  
59  
60

## REFERENCES

- (1) Holm, M. S.; Saravanamurugan, S.; Taarning E. Conversion of sugars to lactic acid derivatives using heterogeneous zeotype catalysts. *Science* **2010**, *328*, 602-605.
- (2) Osmundsen, C. M.; Holm, M. S.; Dahl, S.; Taarning, E. Tin-containing silicates: structure-activity relations. *Proc. R. Soc. A* **2012**, *468*, 2000-2016.
- (3) Moliner, M.; Román-Leshkov, Y.; Davis, M. E. Tin-containing zeolites are highly active catalysts for the isomerization of glucose in water. *Proc. Natl. Acad. Sci. U. S. A.* **2010**, *107*, 6164-6168.
- (4) Román-Leshkov, Y.; Moliner, M.; Labinger, J.; Davis, M. E. Mechanism of glucose isomerization using a solid Lewis acid catalyst in water. *Angew. Chem., Int. Ed.* **2010**, *49*, 8954-8957.
- (5) Bermejo-Deval, R.; Assary, R. S.; Nikolla, E.; Moliner, M.; Román-Leshkov, Y.; Hwang, S.-J.; Palsdottir, A.; Silverman, D.; Lobo, R. F.; Curtiss, L. A. *et al.* Metalloenzyme-like catalyzed isomerizations of sugars by Lewis acid zeolites. *Proc. Natl. Acad. Sci. U. S. A.* **2012**, *109*, 9727-9732.
- (6) Corma, A.; Nemeth, L. T.; Renz, M.; Valencia, S. Sn-zeolite beta as a heterogeneous chemoselective catalyst for Baeyer-Villiger oxidations. *Nature.* **2001**, *412*, 423-425.
- (7) Renz, M.; Blasco, T.; Corma, A.; Fornes, V.; Jensen, R.; Nemeth, L. Selective and shape-selective Baeyer-Villiger oxidations of aromatic aldehydes and cyclic ketones with Sn-beta zeolites and H<sub>2</sub>O<sub>2</sub>. *Chem. – Eur. J.* **2002**, *8*, 4708-4717.



- 1  
2  
3  
4  
5  
6  
7  
8  
9  
10  
11  
12  
13  
14  
15  
16  
17  
18  
19  
20  
21  
22  
23  
24  
25  
26  
27  
28  
29  
30  
31  
32  
33  
34  
35  
36  
37  
38  
39  
40  
41  
42  
43  
44  
45  
46  
47  
48  
49  
50  
51  
52  
53  
54  
55  
56  
57  
58  
59  
60
- (8) Corma, A.; Domine, M. E.; Valencia, S. Water-resistant solid Lewis acid catalysts: Meerwein–Ponndorf–Verley and Oppenauer reactions catalyzed by tin-beta zeolite. *J. Catal.* **2003**, *215*, 294-304.
- (9) Tang, B.; Dai, W.; Wu, G.; Guan, N.; Li, L.; Hunger M. Improved postsynthesis strategy to Sn-beta zeolites as Lewis acid catalysts for the ring-opening hydration of epoxides. *ACS Catal.* **2014**, *4*, 2801–2810.
- (10) Dapsens, P. Y.; Mondelli, C.; Perez-Ramirez, J. Design of Lewis-acid centres in zeolitic matrices for the conversion of renewables. *Chem. Soc. Rev.* **2015**, *44*, 7025-7043.
- (11) Luo, H. Y.; Lewis, J. D.; Roman-Leshkov Y. Lewis acid zeolites for biomass conversion: Perspectives and challenges on reactivity, synthesis, and stability. *Annu. Rev. Chem. Biomol. Eng.* **2016**, *7*, 663–639.
- (12) Boronat, M.; Concepción, P.; Corma, A.; Renz, M.; Valencia S. Determination of the catalytically active oxidation Lewis acid sites in Sn-beta zeolites, and their optimisation by the combination of theoretical and experimental studies. *J. Catal.* **2005**, *234*, 111–118.
- (13) Li, Y.-P.; Head-Gordon, M.; Bell A. T. Analysis of the reaction mechanism and catalytic activity of metal-substituted beta zeolite for the isomerization of glucose to fructose. *ACS Catal.* **2014**, *4*, 1537–1545.
- (14) Kulkarni, B. S.; Krishnamurty, S.; Pal, S. Probing Lewis acidity and reactivity of Sn- and Ti-beta zeolite using industrially important moieties: A periodic density functional study. *J. Mol. Catal. A: Chem.* **2010**, *329*, 36-43.

- 1  
2  
3  
4  
5  
6  
7  
8  
9  
10  
11  
12  
13  
14  
15  
16  
17  
18  
19  
20  
21  
22  
23  
24  
25  
26  
27  
28  
29  
30  
31  
32  
33  
34  
35  
36  
37  
38  
39  
40  
41  
42  
43  
44  
45  
46  
47  
48  
49  
50  
51  
52  
53  
54  
55  
56  
57  
58  
59  
60
- (15) Rai, N.; Caratzoulas, S.; Vlachos, D. G. Role of silanol group in Sn-beta zeolite for glucose isomerization and epimerization reactions. *ACS Catal.* **2013**, *3*, 2294-2298.
- (16) Yang, G.; Pidko, E. A.; Hensen E. J. M. Structure, stability, and Lewis acidity of mono and double Ti, Zr, and Sn framework substitutions in BEA zeolites: A periodic density functional theory study. *J. Phys. Chem. C* **2013**, *117*, 3976–3986.
- (17) Courtney, T. D.; Chang, C.-C.; Gorte, R. J.; Lobo, R. F.; Fan, W.; Nikolakis, V. Effect of water treatment on Sn-BEA zeolite: Origin of 960 cm<sup>-1</sup> FTIR peak. *Microporous Mesoporous Mater.* **2015**, *210*, 69-76.
- (18) Harris, J. W.; Cordon, M. J.; Di Iorio, J. R.; Vega-Vila, J. C.; Ribeiro, F. H.; Gounder, R. Titration and quantification of open and closed Lewis acid sites in Sn-beta zeolites that catalyze glucose isomerization. *J. Catal.* **2016**, *335*, 141–154.
- (19) Otomo, R.; Kosugi, R.; Kamiya, Y.; Tatsumia T.; Yokoi, T. Modification of Sn-beta zeolite: Characterization of acidic/basic properties and catalytic performance in Baeyer–Villiger oxidation. *Catal. Sci. Technol.* **2016**, *6*, 2787–2795.
- (20) Roy, S.; Bakhmutsky, K.; Mahmoud, E.; Lobo, R. F.; Gorte, R. J. Probing Lewis acid sites in Sn-beta zeolite. *ACS Catal.* **2013**, *3*, 573–580.
- (21) Wolf, P.; Valla, M.; Rossini, A. J.; Comas-Vives, A.; Nunez-Zarur, F.; Malaman, B.; Lesage, A.; Emsley, L.; Coperet, C.; Hermans, I. NMR signatures of the active sites in Sn-β zeolite. *Angew. Chem., Int. Ed.* **2014**, *53*, 10179 –10183.

- 1  
2  
3  
4  
5  
6  
7  
8  
9  
10  
11  
12  
13  
14  
15  
16  
17  
18  
19  
20  
21  
22  
23  
24  
25  
26  
27  
28  
29  
30  
31  
32  
33  
34  
35  
36  
37  
38  
39  
40  
41  
42  
43  
44  
45  
46  
47  
48  
49  
50  
51  
52  
53  
54  
55  
56  
57  
58  
59  
60
- (22) Gunther, W. R.; Michaelis V. K.; Caporini, M. A.; Griffin, R. G.; Román-Leshkov, Y. Dynamic nuclear polarization NMR enables the analysis of Sn-beta zeolite prepared with natural abundance  $^{119}\text{Sn}$  precursors. *J. Am. Chem. Soc.* **2014**, *136*, 6219–6222.
- (23) Hwang, S-J.; Gounder, R.; Bhawe, Y.; Orazov, M.; Bermejo-Deval, R.; Davis, M. E. Solid state NMR characterization of Sn-beta zeolites that catalyze glucose isomerization and epimerization. *Top. Catal.* **2015**, *58*, 435–440.
- (24) Kolyagin, Y. G.; Yakimov, A. V.; Tolborg, S.; Vennestrøm, P. N. R.; Ivanova, I. I. Application of  $^{119}\text{Sn}$  CPMG MAS NMR for fast characterization of Sn sites in zeolites with natural  $^{119}\text{Sn}$  isotope abundance, *J. Phys. Chem. Lett.* **2016**, *7*, 1249–1253.
- (25) Gunther, W. R.; Michaelis, V. K.; Griffin, R. G.; Román-Leshkov, Y. Interrogating the Lewis acidity of metal sites in beta zeolites with  $^{15}\text{N}$  pyridine adsorption coupled with MAS NMR spectroscopy. *J. Phys. Chem. C* **2016**, *in press*, DOI: 10.1021/acs.jpcc.6b07811.
- (26) Bermejo-Deval, R.; Gounder, R.; Davis, M. E. Framework and extraframework tin sites in zeolite beta react glucose differently. *ACS Catal.* **2012**, *2*, 2705–2713.
- (27) Gounder, R.; Davis, M. E. Beyond shape selective catalysis with zeolites: hydrophobic void spaces in zeolites enable catalysis in liquid water. *AIChE J.* **2013**, *59*, 3349-3358.
- (28) Boronat, M.; Concepción, P.; Corma, A.; Renz, M. Peculiarities of Sn-beta and potential industrial applications. *Catal. Today.* **2007**, *121*, 39–44.
- (29) Boronat, M.; Concepción, P.; Corma, A.; Navarro, M. T.; Renz, M.; Valencia, S. Reactivity in the confined spaces of zeolites: The interplay between spectroscopy and

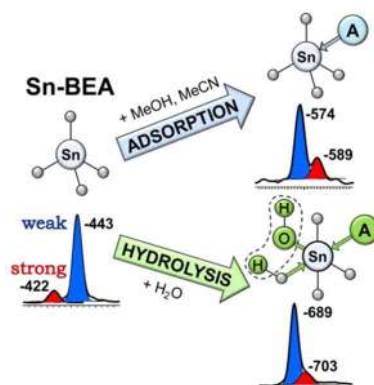
- 1  
2  
3 theory to develop structure–activity relationships for catalysis. *Phys. Chem. Chem. Phys.*  
4  
5 **2009**, *11*, 2876–2884.  
6  
7  
8  
9 (30) Corma, A.; Domine, M. E.; Nemeth, L.; Valencia, S. Al-free Sn-beta zeolite as a catalyst  
10 for the selective reduction of carbonyl compounds (Meerwein-Ponndorf-Verley  
11 reaction). *J. Am. Chem. Soc.* **2002**, *124*, 3194-3195.  
12  
13  
14  
15  
16 (31) Wolf, P.; Valla, M.; Nunez-Zarur, F.; Comas-Vives, A.; Rossini, A. J.; Firth, C.; Kallas,  
17 H.; Lesage, A.; Emsley, L.; Copéret, C. *et al.* Correlating synthetic methods,  
18 morphology, atomic-level structure, and catalytic activity of Sn- $\beta$  catalysts. *ACS Catal.*  
19 **2016**, *6*, 4047–4063.  
20  
21  
22  
23  
24  
25  
26  
27 (32) Lewis, J. D.; Van de Vyver, S.; Crisci, A. J.; Gunther, W. R.; Michaelis, V. K.; Griffin,  
28 R. G.; Román-Leshkov, Y. A continuous flow strategy for the coupled transfer  
29 hydrogenation and etherification of 5-(hydroxymethyl)furfural using Lewis acid zeolites.  
30 *ChemSusChem* **2014**, *7*, 2255 – 2265.  
31  
32  
33  
34  
35  
36  
37 (33) Bermejo-Deval, R.; Orazov, M.; Gounder, R.; Hwang, S-J.; Davis, M. E. Active sites in  
38 Sn-beta for glucose isomerization to fructose and epimerization to mannose. *ACS Catal.*  
39 **2014**, *4*, 2288–2297.  
40  
41  
42  
43  
44  
45 (34) Tolborg, S.; Katerinopoulou, A.; Falcone, D. D.; Sádaba, I.; Osmundsen, C. M.; Davis,  
46 R. J.; Taarning, E.; Fristrup P.; Holm, M. S. Incorporation of tin affects crystallization,  
47 morphology, and crystal composition of Sn-beta. *J. Mater. Chem. A* **2014**, *2*, 20252-  
48 20262.  
49  
50  
51  
52  
53  
54  
55  
56  
57  
58  
59  
60

- 1  
2  
3  
4  
5  
6  
7  
8  
9  
10  
11  
12  
13  
14  
15  
16  
17  
18  
19  
20  
21  
22  
23  
24  
25  
26  
27  
28  
29  
30  
31  
32  
33  
34  
35  
36  
37  
38  
39  
40  
41  
42  
43  
44  
45  
46  
47  
48  
49  
50  
51  
52  
53  
54  
55  
56  
57  
58  
59  
60
- (35) Yakimov, A. V.; Kolyagin, Y. G.; Tolborg, S.; Vennestrøm, P. N. R.; Ivanova, I. I. Accelerated synthesis of Sn-BEA in fluoride media: Effect of H<sub>2</sub>O content in the gel. *New J. Chem.* **2016**, *40*, 4367-4374.
- (36) Chaudhari, K.; Das, T. K.; Rajmohanan, P. R.; Lazar, K.; Sivasanker, S.; Chandwadkar, A. J. Synthesis, characterization, and catalytic properties of mesoporous tin-containing analogs of MCM-41. *J. Catal.* **1999**, *183*, 281–291.
- (37) Massiot, D.; Fayon, F.; Capron, M.; King, I.; Le Calve, S.; Alonso, B.; Durand, J.-O.; Bujoli, B.; Gan, Z.; Hoatson, G. Modelling one- and two-dimensional solid-state NMR spectra. *Magn. Reson. Chem.* **2002**, *40*, 70–76.
- (38) Hammond, C.; Padovan, D.; Al-Nayili, A.; Wells, P. P.; Gibson, E. K.; Dimitratos N. Identification of active and spectator Sn sites in Sn- $\beta$  following solid-state stannation, and consequences for Lewis acid catalysis. *ChemCatChem* **2015**, *7*, 3322 – 3331.
- (39) Bain A. D. Chemical exchange in NMR. *Prog. Nucl. Magn. Reson. Spectrosc.* **2003**, *43*, 63–103.
- (40) Taarning, E.; Saravanamurugan, S.; Holm, M. S.; Xiong, J.; West, R. M.; Christensen, C. H. Zeolite-catalyzed isomerization of triose sugars. *ChemSusChem* **2009**, *2*, 625–627.
- (41) Gunther, W. R.; Wang, Y.; Ji, Y.; Michaelis, V. K.; Hunt, S. T.; Griffin, R. G.; Román-Leshkov, Y. Sn-beta zeolites with borate salts catalyse the epimerization of carbohydrates via an intramolecular carbon shift. *Nat. Commun.* **2012**, *3*, 1109.
- (42) Tolborg, S.; Meier, S.; Sádaba, I.; Elliot, S. G.; Kristensen, S. K.; Shunmugavel, S., Riisager, A.; Fristrup, P.; Skrydstrup, T.; Taarning, E. Tin-containing silicates:

1  
2  
3 Identification of a glycolytic pathway via 3-deoxyglucosone. *Green Chem.* **2016**, *18*,  
4 3360-3369.  
5  
6  
7

- 8  
9 (43) Boronat, M.; Corma, A.; Michael, R. *Catalysis by Lewis acids: Basic Principles for*  
10 *Highly Stereoselective Heterogeneously Catalyzed Cyclization Reactions in Turning*  
11 *Points in Solid-State, Materials and Surface Science: A Book in Celebration of the Life*  
12 *and Work of Sir John Meurig Thomas*; Harris, K. D. M., Edwards, P. P., Eds.; Royal  
13  
14  
15  
16  
17  
18 Society of Chemistry: U.K., 2007.  
19  
20  
21  
22  
23  
24  
25  
26  
27  
28  
29  
30  
31  
32  
33  
34  
35  
36  
37  
38  
39  
40  
41  
42  
43  
44  
45  
46  
47  
48  
49  
50  
51  
52  
53  
54  
55  
56  
57  
58  
59  
60

## TOC Graphic



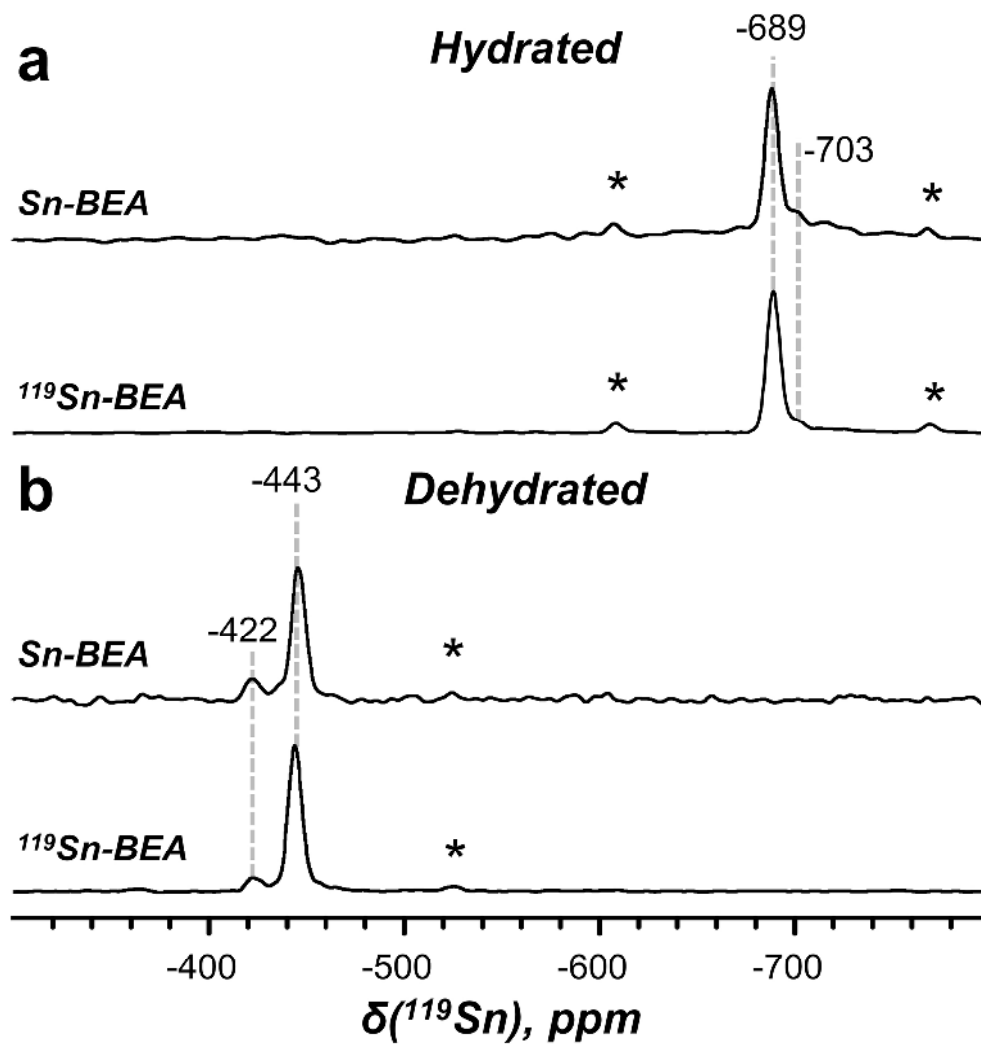
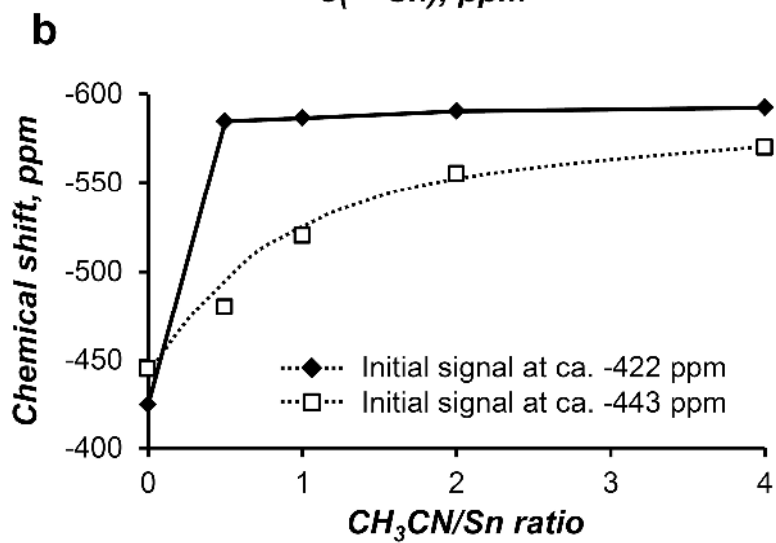
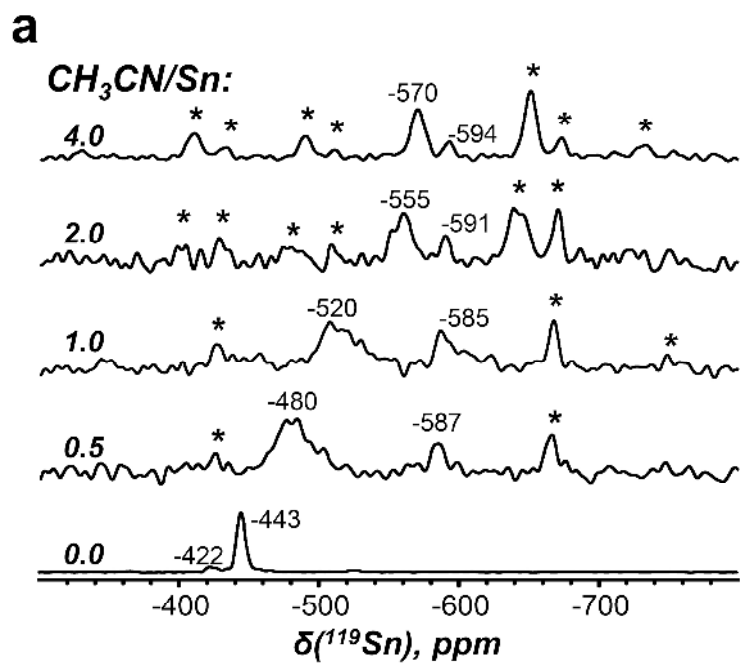


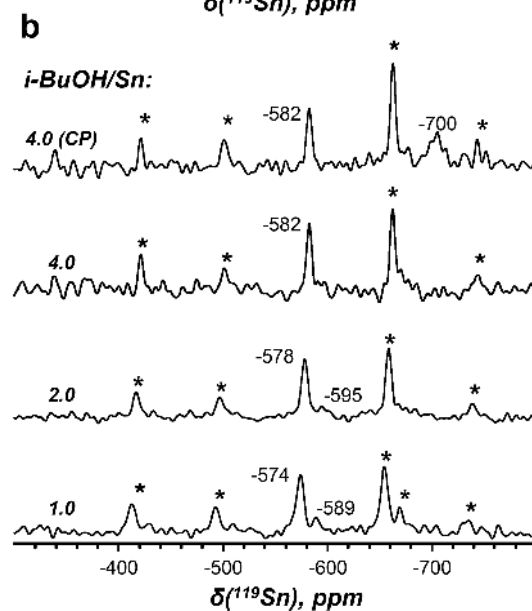
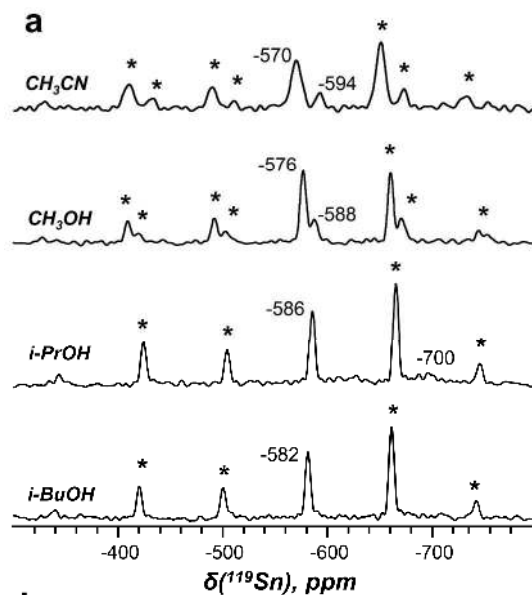
Fig.1

91x97mm (600 x 600 DPI)

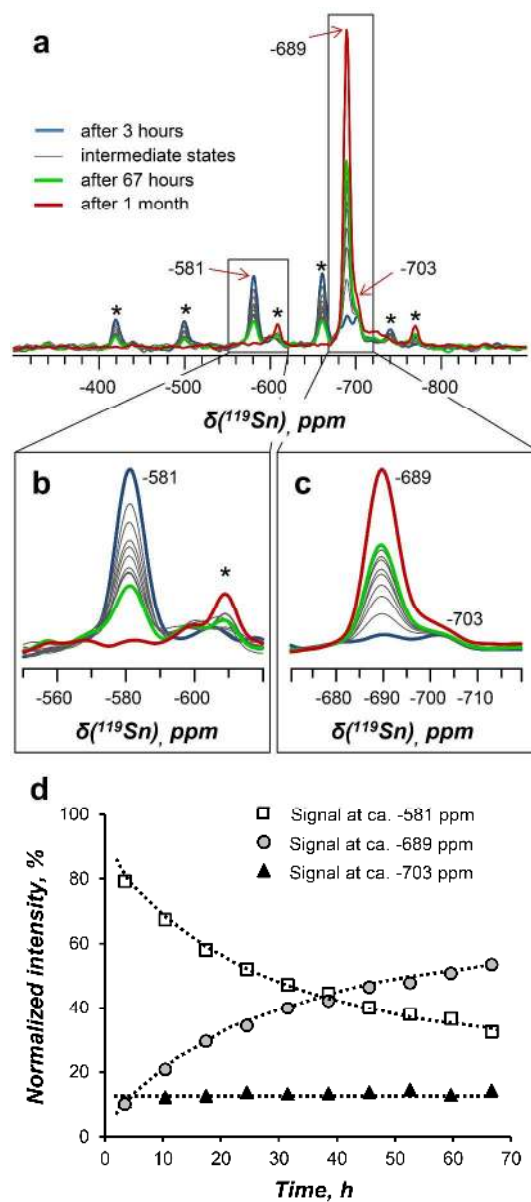




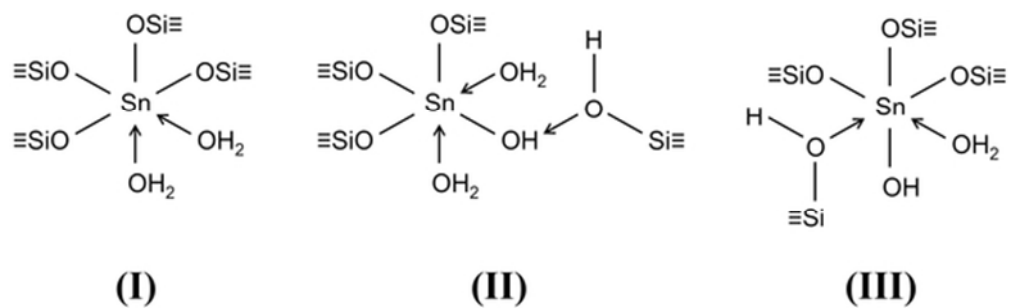
124x183mm (600 x 600 DPI)



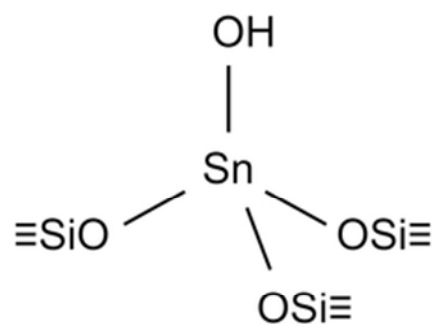
188x416mm (600 x 600 DPI)



189x423mm (600 x 600 DPI)

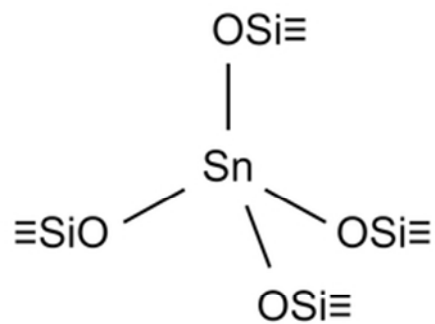


25x7mm (600 x 600 DPI)



20  
21  
22  
23  
24

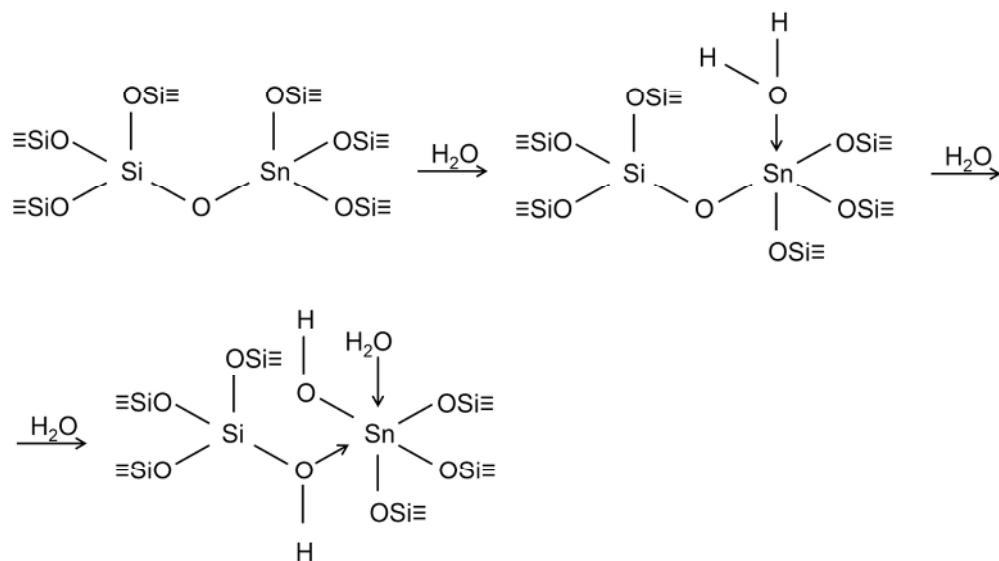
**(IV)**



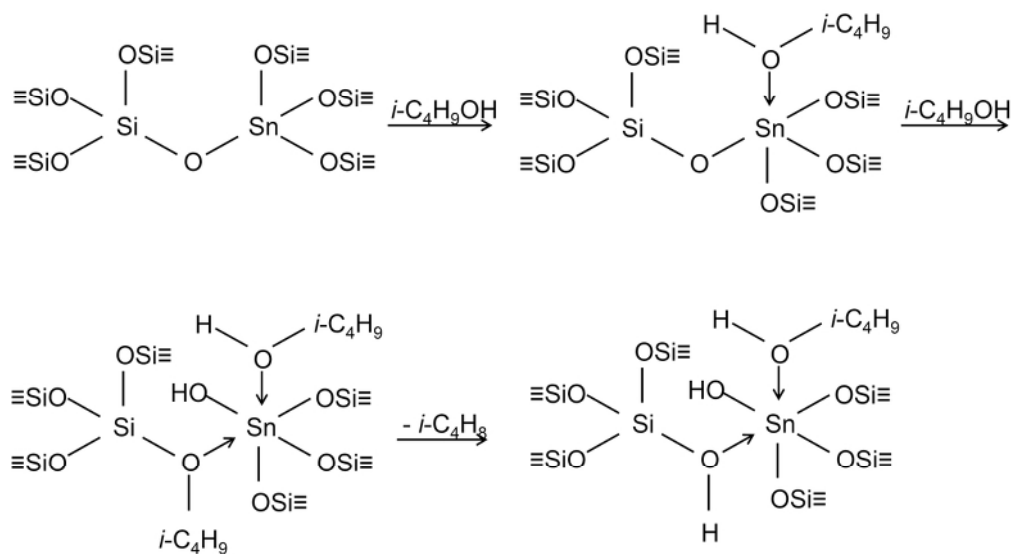
**(V)**

25  
26  
27  
28  
29  
30  
31  
32  
33  
34  
35  
36  
37  
38  
39  
40  
41  
42  
43  
44  
45  
46  
47  
48  
49  
50  
51  
52  
53  
54  
55  
56  
57  
58  
59  
60

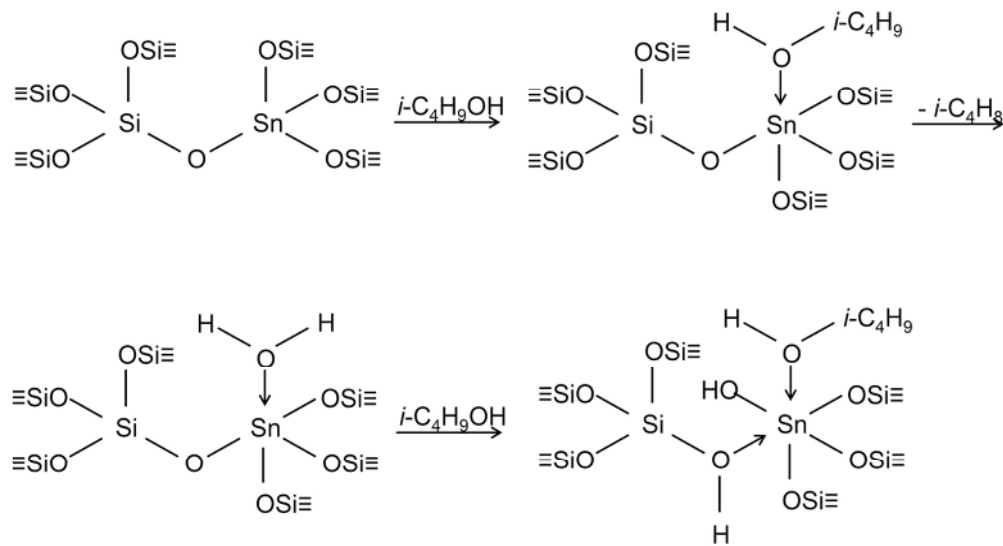
24x11mm (600 x 600 DPI)



48x27mm (600 x 600 DPI)

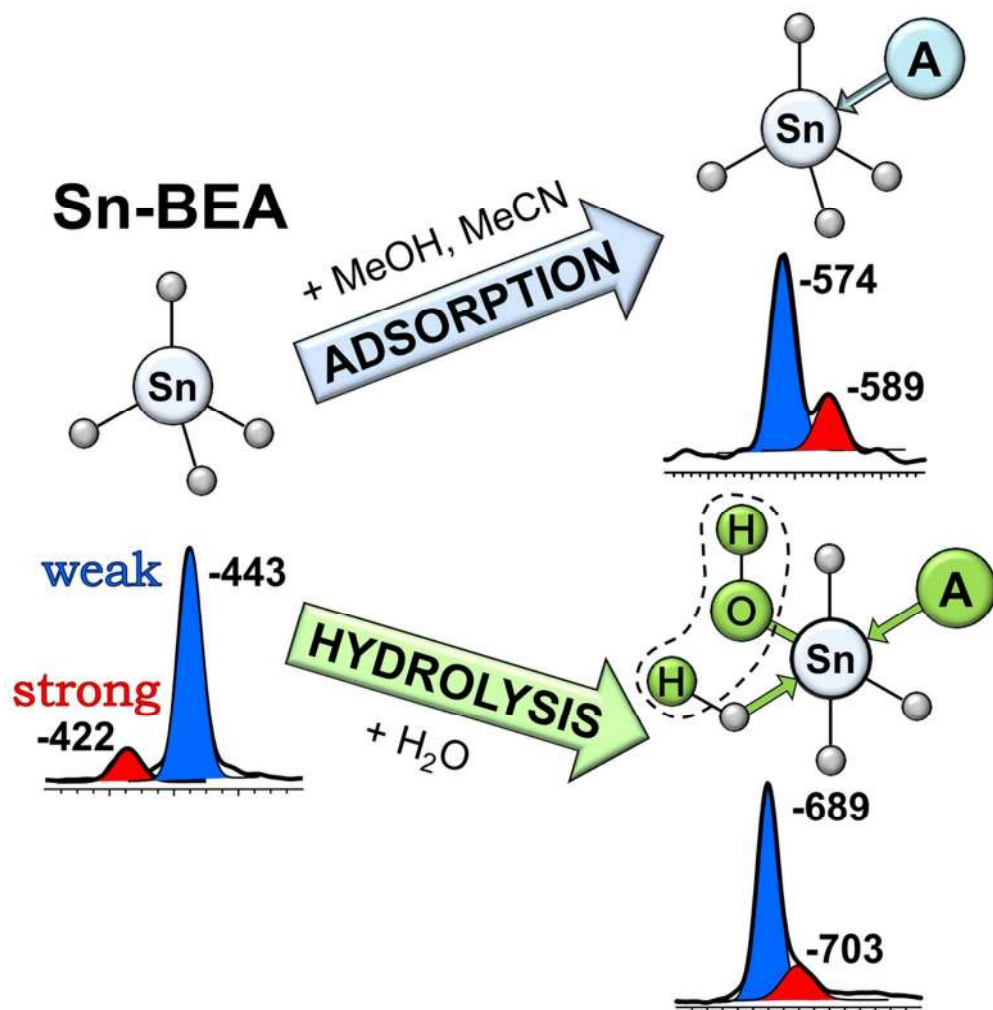


47x26mm (600 x 600 DPI)



47x26mm (600 x 600 DPI)





51x51mm (600 x 600 DPI)